

# **TURBULENCE-INDUCED BUBBLE COLLISION FORCE MODEL DEVELOPMENT AND ASSESSMENT FOR ADIABATIC DISPERSED AIR-WATER TWO-PHASE FLOW WITH THE TWO-FLUID MODEL**

**S. L. Sharma, T. Hibiki, M. Ishii**

School of Nuclear Engineering, Purdue University  
400 Central Dr., West Lafayette, IN 47907-2017, USA  
[sharma55@purdue.edu](mailto:sharma55@purdue.edu), [hibiki@purdue.edu](mailto:hibiki@purdue.edu), [ishii@purdue.edu](mailto:ishii@purdue.edu)

**C. S. Brooks**

Department of Nuclear, Plasma, and Radiological Engineering  
University of Illinois, Urbana-Champaign  
Urbana-Champaign, Urbana, IL 61801, USA  
[csbrooks@illinois.edu](mailto:csbrooks@illinois.edu)

**J.P. Schlegel**

Nuclear Engineering Program, Missouri University of Science and Technology  
301 W 14<sup>th</sup> St, Rolla, MO 65409, USA  
[schlegelj@mst.edu](mailto:schlegelj@mst.edu)

**Y. Liu**

Nuclear Engineering Program, Department of Mechanical Engineering  
Virginia Polytechnic Institute and State University  
Blacksburg, VA 24061, USA  
[liu130@vt.edu](mailto:liu130@vt.edu)

**J.R. Buchanan, Jr.**

Bechtel Marine Propulsion Corporation, Bettis Laboratory  
814 Pittsburgh-McKeesport Blvd, West Mifflin, PA 15122, USA  
[jack.buchanan@unnpp.gov](mailto:jack.buchanan@unnpp.gov)

## **ABSTRACT**

The prediction capability of the two-fluid model for gas-liquid dispersed two-phase flow depends on the accuracy of the closure relations for the interfacial forces. In previous studies of two-phase flow Computational Fluid Dynamics (CFD), interfacial force models for a single isolated bubble has been extended to disperse two-phase flow assuming the effect in a swarm of bubbles is similar. Limited studies have been performed investigating the effect of the bubble concentration on the lateral phase distribution. Bubbles, while moving through the liquid phase, may undergo turbulence-driven random collision with neighboring bubbles without significant coalescence. The rate of these collisions depends upon the bubble approach velocity and bubble spacing. The bubble collision frequency is expected to be higher in locations with higher bubble concentrations, i.e., volume fraction. This turbulence-driven random collision causes the diffusion of the bubbles from high concentration to low concentration. Based on experimental observations, a phenomenological model has been developed for a “turbulence-induced bubble collision force” for use in the two-fluid model. For testing the validity of the model, two-phase flow data measured at Purdue University are utilized. The geometry is a 10 mm x 200 mm cross section

channel. Experimentally, non-uniform inlet boundary conditions are applied with different sparger combinations to vary the volume fraction distribution across the wider dimension. Examining uniform and non-uniform inlet data allows for the influence of the volume fraction to be studied as a separate effect. The turbulence-induced bubble collision force has been implemented in ANSYS CFX. The assessment results show agreement with the measured data, correctly capturing the redistribution of volume fraction downstream with uniform and non-uniform inlet profiles. In particular, for the non-uniform data, the transverse redistribution of volume fraction at downstream locations is captured. This signifies the importance of bubble-bubble collision phenomena in correctly predicting volume fraction distributions.

## **KEYWORDS**

Bubble collision based diffusion, Interfacial force, Two-fluid model, Turbulence, CFD

## **1. INTRODUCTION**

In recent years, Computational Fluid Dynamics (CFD) has emerged as a very useful tool for engineers and scientists, providing valuable information on the temporal and spatial distribution of key variables in a flow field. The existing commercial CFD codes can be applied with confidence to solve a variety of single-phase flow problems, however considerable research effort is still necessary before CFD can be applied to the study of gas-liquid two-phase flows with the same level of confidence. While Direct Numerical Simulation (DNS) is still beyond reach for industrial flow problems involving significant void fraction due to excessive computational requirements, an Eulerian-Eulerian approach (two-fluid model) is widely used and considered well suited for industrial scale two-phase flow problems [1]. Present commercial two-phase CFD tools already have Eulerian-Eulerian modeling capability using the two-fluid model, which was developed by Ishii [1-3] by time averaging the instantaneous transport equations (continuity, momentum and energy) for each phase. The time averaging results in interfacial transfer terms in the two-fluid model which require closure relations. The prediction capability of the two-fluid model relies heavily on the accuracy of these closure relations. The interfacial transfer terms are directly proportional to interfacial area concentration. Therefore, an accurate model for the interfacial area concentration is necessary for detailed treatment of the phase interactions.

Most two-phase flow conditions may include the spherical, distorted, cap, slug and churn-turbulent bubbles. Such differences of bubbles in size and shape cause substantial differences in their transport phenomena due to the variations in interfacial forces and the particle interaction mechanisms. In view of their transport characteristics, the bubbles can be classified into two major groups. The spherical and distorted bubbles are considered as the Group-1 bubbles, while the Group-2 bubbles include the cap, slug and churn-turbulent bubbles [1,4]. Therefore, the 3-D three-field two-fluid model with two-group Interfacial Area Transport Equation (IATE) has been selected as the framework implemented in the commercial CFD code ANSYS CFX. This framework can serve as common framework of two-fluid model along with a single set of constitutive relations which can predict the wide range of two-phase flow conditions starting from bubbly to churn-turbulent flow. The two-group Interfacial Area Transport Equation (IATE) is utilized here to predict the dynamic structure of two phase flows by taking into account various possible bubble coalescence and breakup mechanism. Details of the two-fluid model and IATE along with closure relations can be found in past work [1]. In the present work, the focus is on bubbly gas-liquid flow.

In case of adiabatic two-phase flow, the interfacial force terms in the momentum equation are generally considered to include drag force, lift force, wall force, and dispersion force for bubbles by liquid eddies.

A thorough literature survey has been done for the best available hydrodynamic models. The best available model chosen and used for the current research simulations are listed in Table I. Generally, the existing interfacial models in literature have been derived for a single isolated bubble and have been extended to disperse two-phase flow assuming the effect in a swarm of bubbles is similar. However, it is intuitive that a bubble in a swarm while moving in a transverse direction (either from channel center to the wall region or vice versa), undergoes collisions with other bubbles. Limited studies have been performed investigating the effect of the bubble concentration on the lateral phase distribution. It is important to model this phenomenon and assess its effect. The next section discusses the modeling approach taken and assumptions in detail for the “turbulence-induced bubble collision force”.

**Table I. Summary of Interfacial Forces and Constitutive Relations for Momentum Equation Applied in Benchmark Cases**

Interfacial Forces	Phases	Nature	Coefficient
Drag Force	Gas and Liquid	Interfacial force	Ishii and Zuber (1979) [5]
Wall Lubrication Force	Gas and Liquid	Interfacial force	Antal et al. (1991) [6] $C_{w1} = -0.01, C_{w2} = 0.05$
Lift force	Gas and Liquid	Interfacial force	Hibiki and Ishii (2007) [7]
Turbulent dispersion force	Gas and Liquid	Interfacial force	Bertodano (1992) [8] $C_{TD,1} = 0.25$
Bubble-induced turbulence	Liquid	Reynolds stress	Sato et al. (1981) [9] $C_{Sato,G1} = 0.6$

## 2. MODEL DEVELOPMENT

It is hypothesized that strong bubble diffusion happens due to the relatively dense packing of bubbles, which increases the collision frequencies among bubbles. As a result of random collisions (without significant coalescence), bubbles are pushed from higher concentration to lower concentration as there are more collisions on the higher concentration side, i.e., the net collision force should act opposite, and be proportional to, the gradient of bubble number density,  $\nabla n_b$ , or void fraction,  $\nabla \alpha_g$ . The motion of the bubbles is driven by the turbulent eddies. The net collision force is proportional to the momentum of bubbles undergoing collision divided by the time interval of collision. The virtual mass effect should also be considered for the momentum of bubbles. The formulation of the “turbulence-induced bubble collision force” is as follows:

The force per unit volume of the bubbly mixture is written as

$$M^C \propto -(\nabla n_b \cdot D_E) \frac{m_{b1} v_{b1}}{\Delta t_c} P_c \propto -(\nabla n_{b1} \cdot D_E) \frac{m_{b1} v_{b1}^2}{L_t} P_c \quad (1)$$

where the bubble concentration, i.e. number of bubbles per unit volume mixture, is

$$n_b = \frac{\alpha_g}{V_{bubble}}. \quad (2)$$

The virtual mass of bubble undergoing collision is

$$m_b \approx \frac{1}{2} V_{bubble} \rho_f \quad (3)$$

The bubble volume undergoing collision is  $V_{bubble}$ , the continuous phase density is  $\rho_f$ , and the distance between the center of two bubbles is

$$D_E \approx \frac{D_b}{\alpha_g^{1/3}}, \quad (4)$$

which can also be seen as an effective diameter of the mixture volume. Assuming isotropic turbulence, the bubble approach velocity is proportional to the liquid fluctuating velocity which is related to length scale,  $D_b$  [10],

$$v_b \approx u_t \approx (\varepsilon D_b)^{1/3}, \quad (5)$$

and the mean travelling distance is

$$L_t \approx D_E - \gamma D_b \propto \frac{D_b}{\alpha_g^{1/3}} \{1 - \gamma' \alpha_g^{1/3}\} \propto \frac{D_b}{\alpha_g^{1/3}} \left\{ 1 - \left( \frac{\alpha_g}{\alpha_{g,max}} \right)^{1/3} \right\}. \quad (6)$$

In the above definition of the mean traveling distance,  $\gamma'$  is the approximation factor which represents asymptotic value of  $\alpha_{g,max}^{1/3}$ . This formulation makes sure that when void fraction approaches the dense packing limit of  $\alpha_{g,max}$ , the mean travelling distance for the colliding bubbles should approach zero. Several of these definitions can be observed graphically in Fig. 1.

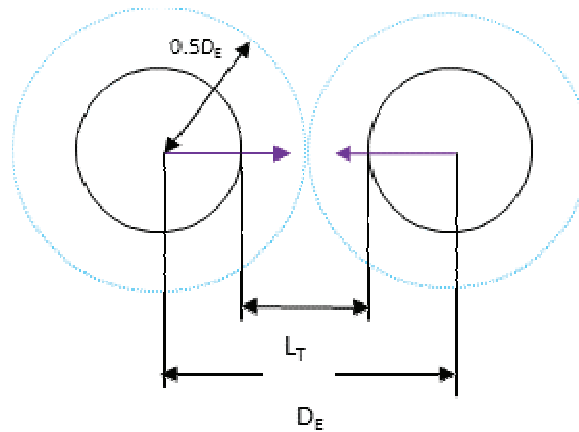


**Figure 1. Geometric Definitions of Two Approaching Bubbles**

Assuming hexagonal close packing, the collision probability can be given as

$$P_C \propto \frac{D_b^2}{D_E^2}. \quad (7)$$

In this expression, it should be taken in to account that the collision probability should approach 1 when void fraction reaches  $\alpha_{g,max}$  so that

$$P_C \propto \left( \frac{\alpha_g}{\alpha_{g,max}} \right)^{2/3}. \quad (8)$$

After substituting the respective definitions, approximations and simplifying further, the bubble collision force per unit volume mixture becomes

$$M^C = - \left( K \left( \frac{\nabla \alpha}{V_{bubble}} \right) \left( \frac{D_b}{\alpha_g^{1/3}} \right) \frac{V_{bubble} \rho_f \alpha_g^{2/3} u_t^2}{\frac{D_b}{\alpha_g^{1/3}} \left\{ 1 - \left( \frac{\alpha_g}{\alpha_{g,max}} \right)^{1/3} \right\}} \left( \frac{\alpha_g}{\alpha_{g,max}} \right)^{2/3} \right) \quad (9)$$

So, finally, the formulation becomes

$$M^C = - \left( K \frac{\rho_f u_t^2}{2 \alpha_{g,max}^{2/3}} \right) f(\alpha_g) \nabla \alpha \quad (10)$$

where,  $\alpha_{g,max} \approx 0.62$  is the dense packing limit for smaller Group-1 bubbles and

$$f(\alpha_g) = \alpha_g^{2/3} \left[ 1 - \left( \frac{\alpha_g}{\alpha_{g,max}} \right)^{1/3} \right]^{-1} \quad (11)$$

represents the dependence of turbulence-induced bubble collision force on the concentration of the bubbles. As shown in Fig. 2, this term increases as void fraction increases indicating that as bubble concentration increases, there would be more collisions and the force becomes stronger. Also, the dependence of the colliding bubble velocity term on turbulence parameters in the above formulation represents the effect of the increase in turbulence on the diffusion of the bubbles with increasing liquid volumetric flux. The bubble size in Eq. (5) is taken approximately as bubble Sauter mean diameter which is calculated from void fraction and interfacial area concentration.

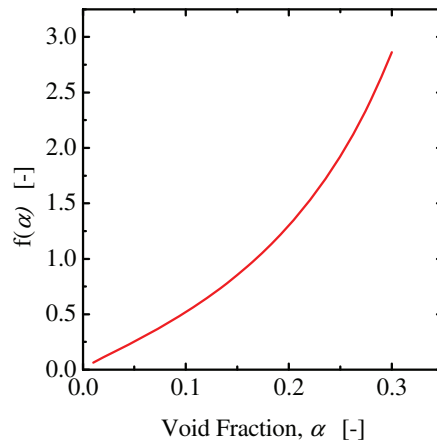


**Figure 2. Variation of  $f(\alpha_g)$  with Void Fraction**

The above collision force model, Eq. (10), gives  $K$  as a proportionality constant to absorb the approximations assumed in the modeling process. It was found that  $K=1$  gives reasonable diffusion force for small group-1 bubbles. The next step is assessing the model against highly reliable and accurate two phase flow measured data. For this purpose, two-phase flow data measured at Purdue University are utilized. What follows next is the brief description of the experimental setup used for the measured data.

### 3. EXPERIMENTAL SETUP AND TEST CONDITIONS

The experimental database used for the present study was performed in a narrow rectangular channel geometry. Figure 3(a) shows the schematic of the experimental loop. The test loop was designed to perform adiabatic air-water two-phase flow experiments in bubbly, cap-turbulent, and churn-turbulent flow regimes at room temperature and close to atmospheric conditions. The experimental loop includes two phase flow injection unit, test section, upper plenum, and the liquid and gas delivery system. The test section had cross-sectional dimension of 200mm (x-direction) by 10mm (y-direction) and was approximately 3m in height. It was made of transparent acrylic for optimal flow visualization. The unique design of the two-phase mixture injection unit allows the test loop to be capable of controlling both the gas and liquid flow rates to desired combinations by manipulation of manifolding valves. The four-sensor conductivity probe ports are installed on the flow duct gap (y-direction) at  $z/D_H=35$  (Port 2), 88 (Port 4) and 142 (Port 6) away from the top of the two-phase mixture injection unit. Detailed local data including void fraction, interfacial area concentration, bubble velocity and Sauter mean diameter were acquired by traversing the probe at each instrumentation port location. Details of the experimental loop can be seen in [11]. Flow conditions selected for the validation is shown on the flow regime map in Fig. 3(b) and details are included in Table II. These conditions were created by injecting gas and liquid in different fashion with the help of spargers as shown in Table II. Average bubble sizes in this set of experimental data range from 2 to 5mm.

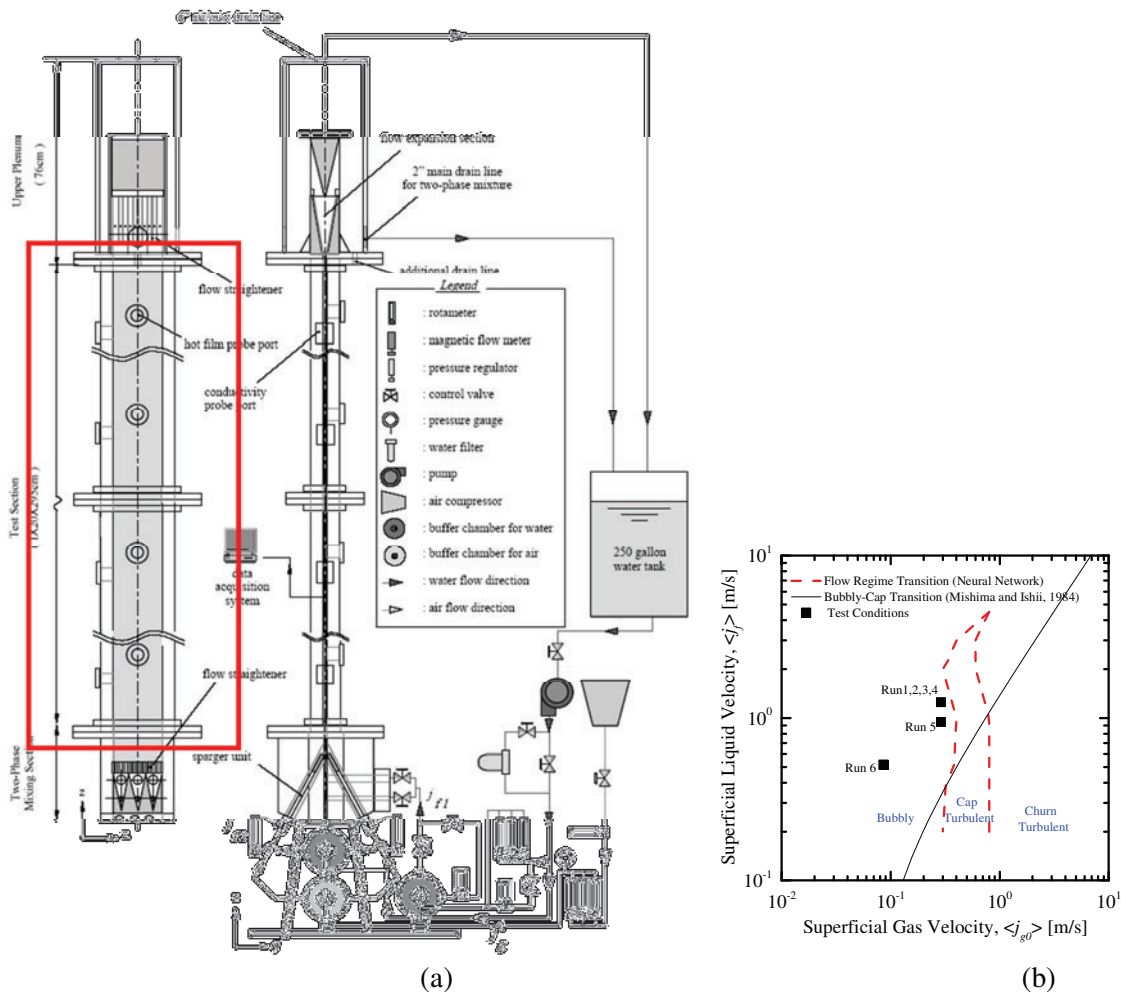
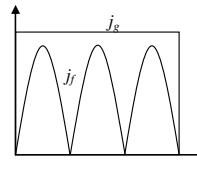
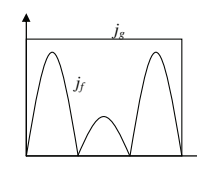
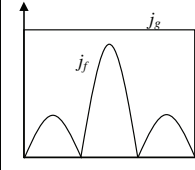
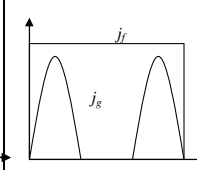
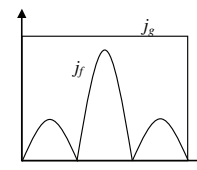
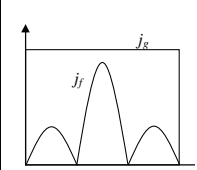


Figure 3. (a) Schematic Diagram of Experimental Facility [11] (b) Test conditions in a  $j_g$ - $j_f$  map.

**Table II. Summary of Test Conditions**

Run 1	Run 2	Run 3	Run 4	Run 5	Run 6
$\langle j_{g,0} \rangle = 0.289$ m/s $\langle j_l \rangle = 1.25$ m/s	$\langle j_{g,0} \rangle = 0.289$ m/s $\langle j_l \rangle = 1.25$ m/s	$\langle j_{g,0} \rangle = 0.289$ m/s $\langle j_l \rangle = 1.25$ m/s	$\langle j_{g,0} \rangle = 0.295$ m/s $\langle j_l \rangle = 1.25$ m/s	$\langle j_{g,0} \rangle = 0.289$ m/s $\langle j_l \rangle = 0.943$ m/s	$\langle j_{g,0} \rangle = 0.295$ m/s $\langle j_l \rangle = 1.25$ m/s
					
Uniform $j_f$ Profile	Double Side $j_f$ Profile	Center $j_f$ Profile	Double Side $j_g$ Profile	Center $j_f$ Profile	Center $j_f$ Profile

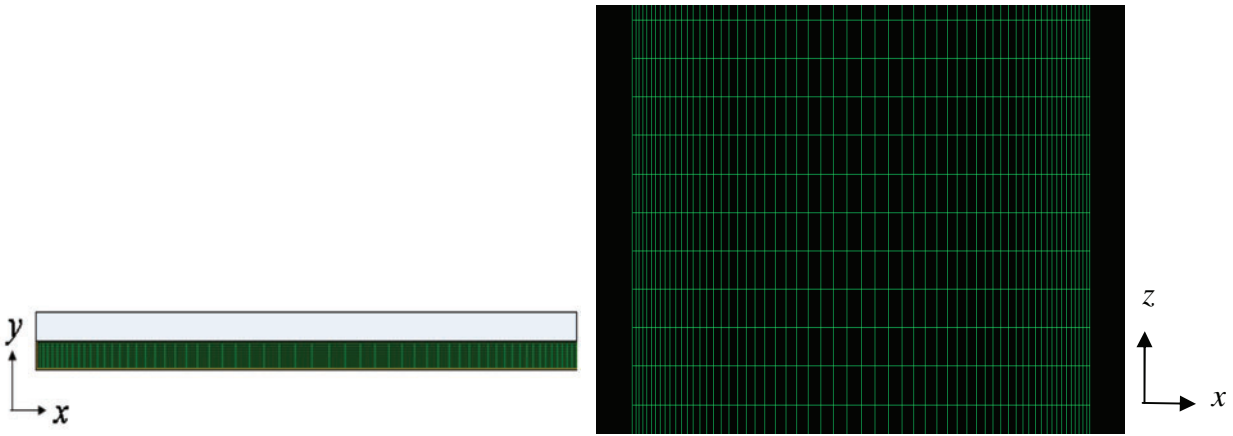
#### 4. PREPARATION OF BENCHMARK

The preparation of benchmark starts with the geometry and mesh generation. The highlighted region in Fig.3(a) shows the geometry selected for the mesh generation. The focus is on the test section which includes local instrumentation ports. The geometry is a rectangular duct that has dimensions of 200mm×10mm×2340mm. The generation of the calculation domain is focused on a half of the whole cross sectional duct as shown in Fig. 4, to save computation time based on the symmetric conditions. Based on a mesh sensitivity study it was found that hexahedral mesh configuration of 60×10×162 with total 97,200 computational cells was sufficient to give details of the phase distribution in the present geometry. The mesh with relatively fine cells near the wall region is used to capture the high gradient of two-phase flow parameters near the wall. While selecting the mesh size near the wall, the near wall spacing was selected such that  $y^+ > 30$  as the log law of the wall has been used for the present simulations.

The inlet boundary conditions are based on information at the first measurement section (Port 2,  $z/D_h = 34.76$ ) due to the limited information at the inlet of the test section. The local measurement data of void fraction, interfacial area concentration, and gas velocity are used to specify inlet boundary conditions and domain initialization. The liquid velocity profile is derived from the gas velocity profile by subtracting the slip velocity. In the short gap, y-direction, 1/7<sup>th</sup> power law variation is assumed for the liquid velocity profile. A constant pressure is used for the outlet boundary condition. The free slip wall boundary condition is specified for the gas phase. The no slip wall boundary condition is used for the liquid phase, however the scalable wall function is applied for the near wall treatment [12]. The  $k - \epsilon$  turbulence model is used for the turbulence model [13- 23].

In the current benchmark study, ANSYS CFX (v. 14.0, ANSYS, Inc., Canonsburg, PA) with a new customized executable solver with the IATE incorporated has been used for the three-field two-fluid model simulations [24] (aka Eulerian-Eulerian approach). ‘High Resolution’ is selected as the advection scheme and  $10^{-5}$  is taken as the Root Mean Square (RMS) residual target for convergence of the simulation. The coupled void fraction option under ‘Multiphase Control’ options has been used in the simulations. The time step size was selected on a case-by-case basis to obtain faster convergence.

Due to high aspect ratio (20:1) and narrow gap size (G=10mm in y-direction) of the rectangular channel considered for present study, the phase distribution in the y-direction is relatively uniform compared to that in the x-direction. Therefore the local results are averaged in y-direction over gap size (G=10mm) for comparing the simulation results with the experimental.



(a) Transverse Mesh

(b) Axial Mesh

Figure 4. Mesh used for Flow Conditions with Non-Uniform Inlet Conditions

## 5. MODEL ASSESSMENT RESULTS

For the assessment of turbulence induced bubble collision force, it is important to consider the bubbly flow conditions with non-uniform inlet conditions. The six test conditions considered have resulted from different injection methods at the inlet as shown in Table II. The first test case to be discussed here is Run 1, which is primarily a one group bubbly case and located near bubbly to cap-turbulent transition as shown in Fig. 3(b). The measured void fraction profile at Port-2 which was used as inlet boundary condition for the void fraction has high non-uniformity resulting from injection effect of spargers (shown in Fig. 5), whereas at Port 4 and Port 6, the measured void profile is more or less flat. This case is a good test for assessing the diffusion force model for small Group-1 bubbles. First, the CFX benchmarking simulation was carried out with bubble collision force and with applicable interfacial forces included in Table I. As can be seen from Fig. 5, with the existing set of interfacial force models, in the absence of bubble collision diffusion force, the trends are not captured. Increasing the coefficient of the bubble dispersion force [8] doesn't change the result much. Fig. 6 shows the phase distribution result, with addition of turbulence-induced bubble collision force model. As can be seen, the void distribution at Port 4 and Port 6 are better predicted.

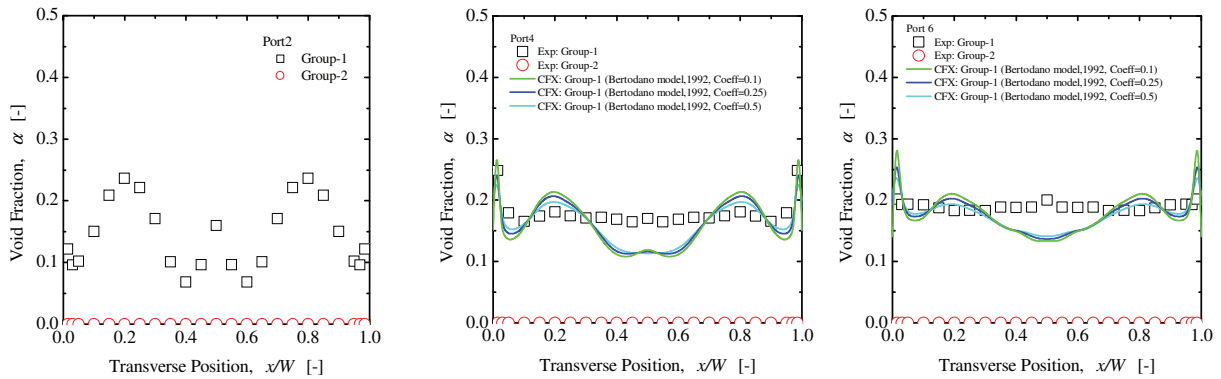
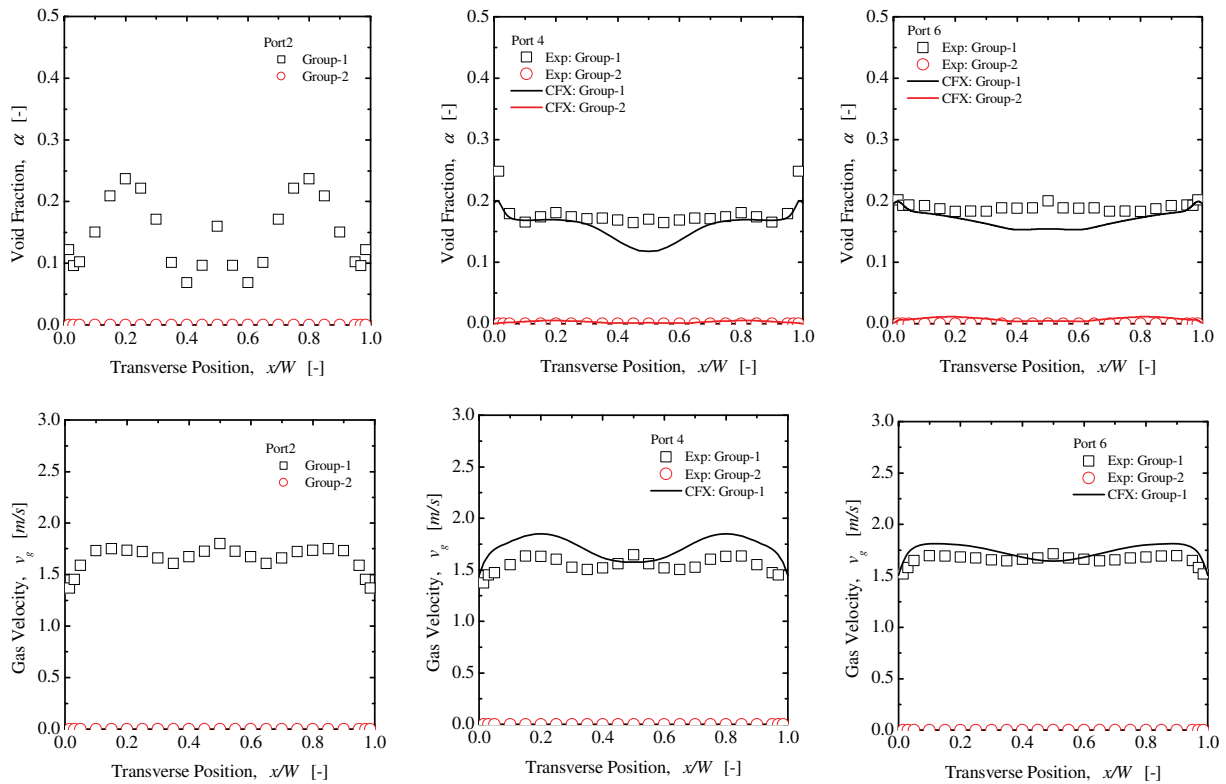
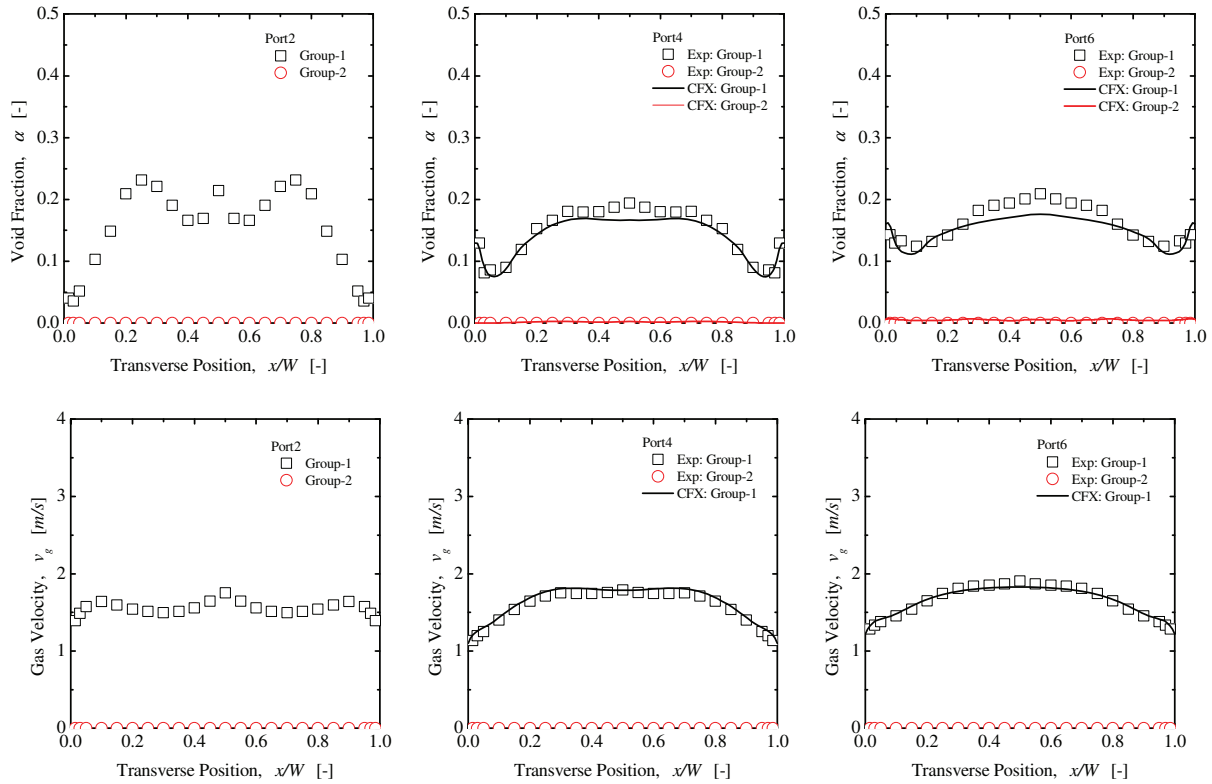


Figure 5. Local Phase Distribution at Port 2 (inlet profile), Port 4 and Port 6 without Bubble Collision Force (Run 1)



**Figure 6. Local Phase Distribution at Port 4 and Port 6 with Bubble Collision Force (Run 1)**

To further assess the bubble collision diffusion force model the benchmark simulations were run including diffusion force model for other test cases (Run 2, 3, 4, 5 and 6). These test cases have non-uniform inlet conditions in the form of either center peaked or wall peaked inlet void profile generated with the help of spargers as shown in the Table II. The phase distribution results predicted by CFX in comparison with the measurement for Run 2, 3, 4, 5 and 6 are shown in Figure 7, 8, 9, 10, 11 respectively. Inlet phase distribution at Port 2 clearly carries the signature of the injection method, but due to the combined action of interfacial forces, the phase distribution changes along the flow path. Wall force and lift force mainly play an important role in the phase distribution near the wall region due to high liquid velocity gradients. In the bulk region of the channel, the bubble diffusion force model disperses the bubbles from the region of high void gradient. For Run 3 (Fig. 8), the gas velocity is over predicted relative to the experimental data. For Run 5 (Fig. 10), the gas velocity is over predicted and void fraction under predicted relative to the experimental data. Both of these cases are center-peaked liquid velocity injection and significant changes in bubble Sauter mean diameter are observed in the experiment, more so than the other runs considered. This will be investigated in greater detail. Overall, the combined action of the interfacial forces listed in Table I and bubble collision diffusion force results in a good prediction of phase distribution for all six test conditions.



**Figure 7. Local Phase Distribution at Port 4 and Port 6 with Bubble Collision Force (Run 2)**

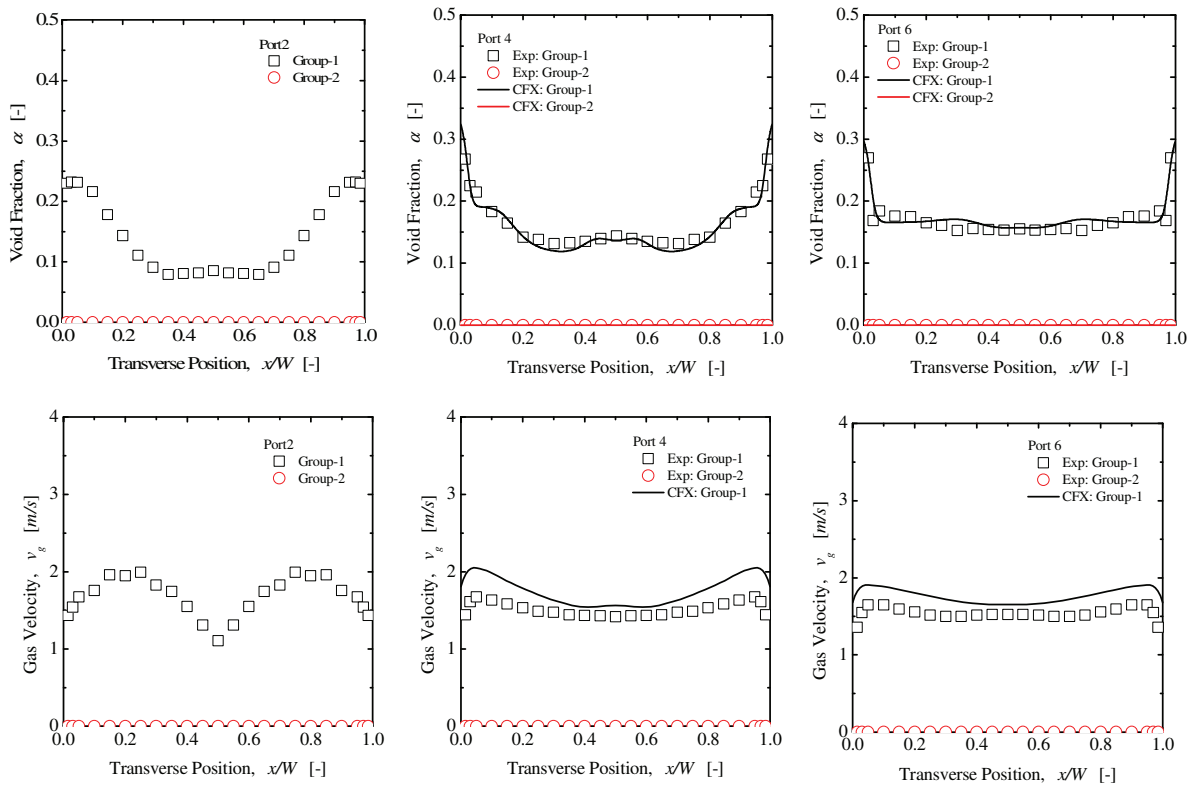


**Figure 8. Local Phase Distribution at Port 4 and Port 6 with Bubble Collision Force (Run 3)**

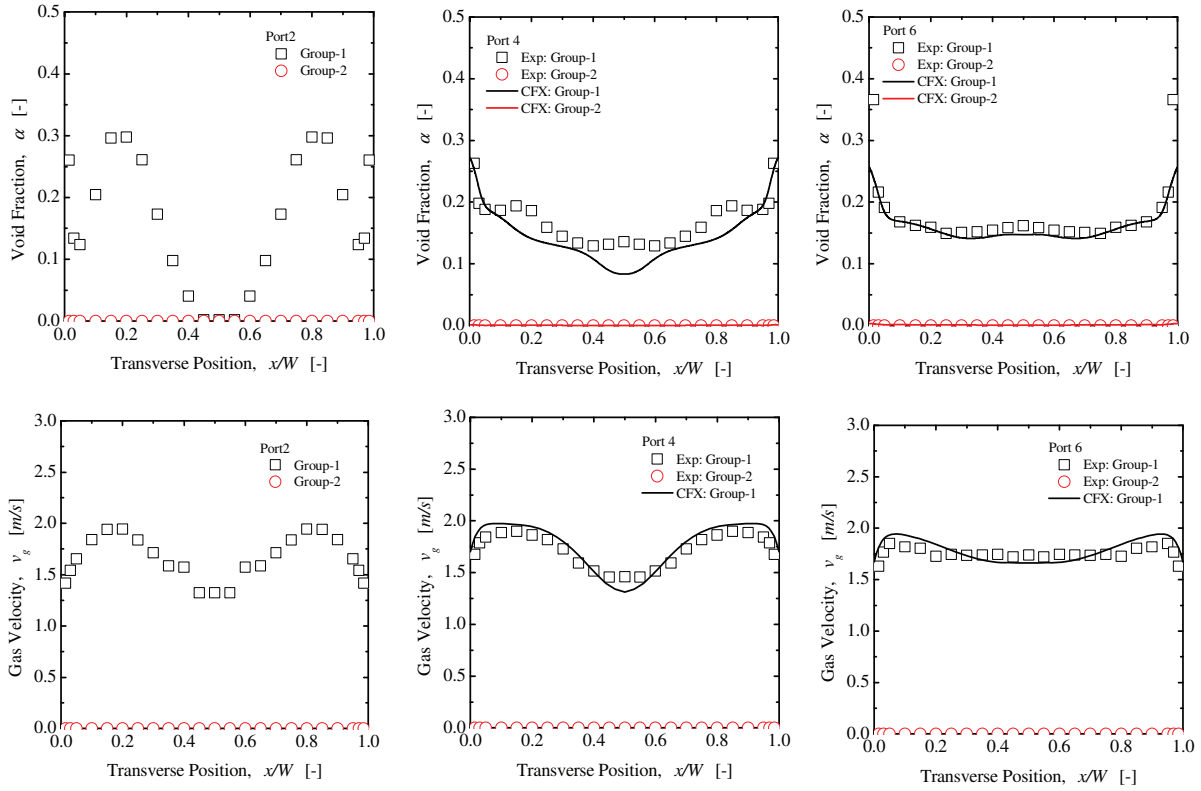


**Figure 9. Local Phase Distribution at Port 4 and Port 6 with Bubble Collision Force (Run 4)**

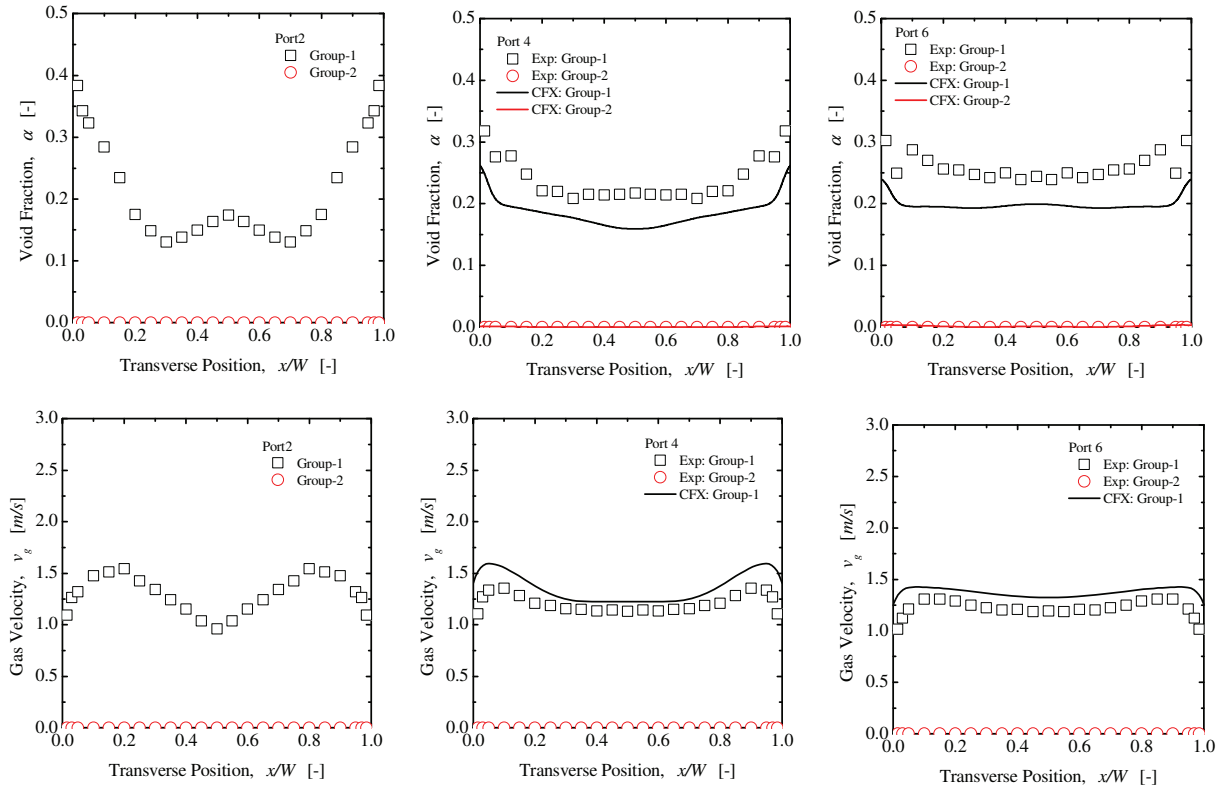


**Figure 10. Local Phase Distribution at Port 4 and Port 6 with Bubble Collision Force (Run 5)**

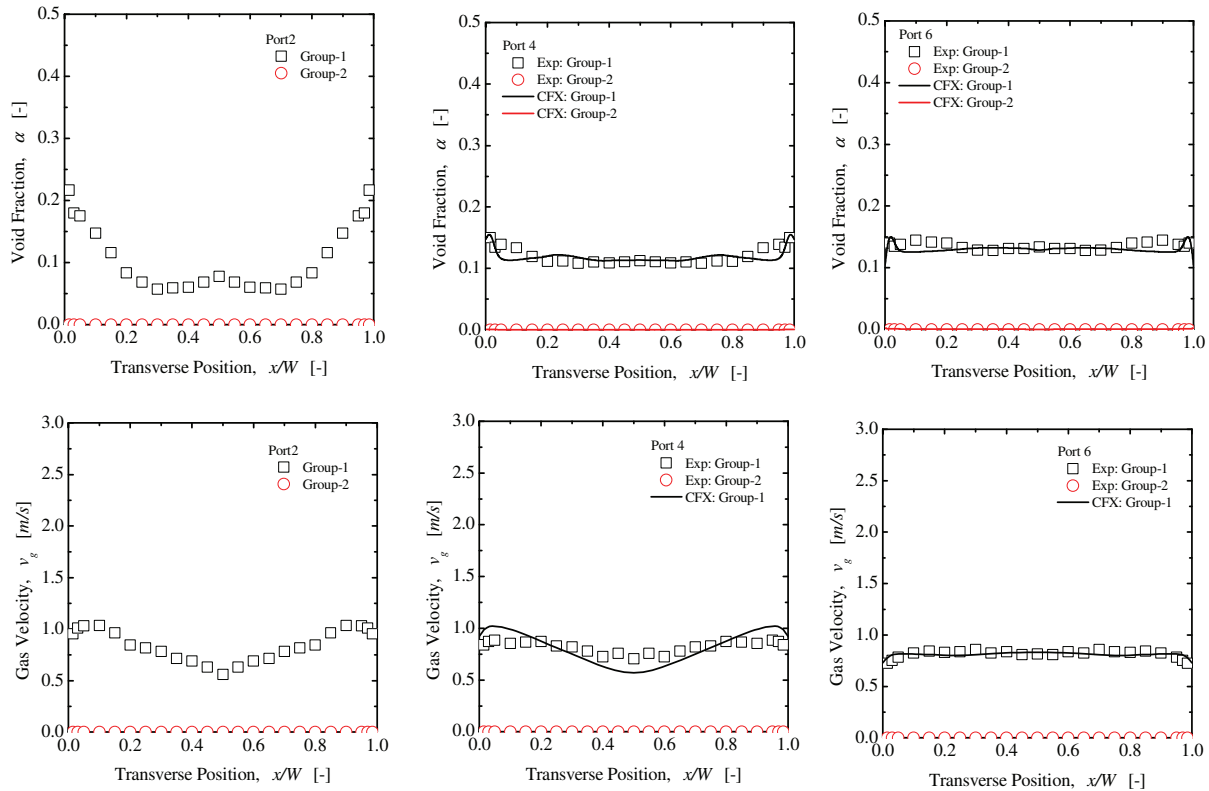


**Figure 11. Local Phase Distribution at Port 4 and Port 6 with Bubble Collision Force (Run 6)**

## 6. CONCLUSIONS

In this study, the three-field two-fluid model with two-group IATE was prepared in a commercial 3-D CFD code, ANSYS CFX. Dynamic evaluation of the interfacial structure was considered by implementing the two-group IATE with various bubble interaction mechanisms (coalescence and break up) as the source and sink terms into the code using user defined functions and subroutines. Interfacial forces which were found important *i.e.*, drag force [5], wall lubrication force [6], the lift force with a physics-based lift coefficient [7], turbulent dispersion force [8], were also implemented. A phenomenological model for the turbulence-induced bubble collision diffusion force was developed and assessed against the non-uniform inlet conditions (skewed void profile at the inlet). The phase distribution results predicted by the model showed good agreement with the measured data.

### Notice

This report was prepared as an account of work sponsored by an agency of the United States Government. Neither the United States Government nor any agency thereof, nor any of their employees, nor any of their contractors, subcontractors or their employees, makes any warranty, express or implied, or assumes any legal liability or responsibility for the accuracy, completeness, or any third party's use or the results of such use of any information, apparatus, product, or process disclosed, or represents that its use would not infringe privately owned rights. Reference herein to any specific commercial product, process, or service by trade name, trademark, manufacturer, or otherwise, does not necessarily constitute or imply its endorsement, recommendation, or favoring by the United States Government or any agency thereof or its

contractors or subcontractors. The views and opinions of authors expressed herein do not necessarily state or reflect those of the United States Government or any agency thereof.

## REFERENCE

1. M. Ishii and T. Hibiki, *Thermo-fluid dynamics of two-phase flow*. Springer, New York (2011).
2. M. Ishii., *Thermo-fluid dynamic theory of two-phase flow*. Eyrolles, Paris (1975).
3. M. Ishii and K. Mishima, “Two-fluid model and hydrodynamic constitutive relations”. *Nucl. Eng. Des.* **82**, pp. 107-126 (1984).
4. X. Sun, *Two-group interfacial area transport equation for a confined test section*, Ph.D. Thesis, Purdue University, West Lafayette, IN (2001).
5. M. Ishii and N. Zuber, “Drag coefficient and relative velocity in bubbly, droplet or particulate flows”. *AIChE J.* **25**, pp.843 (1979).
6. S. P. Antal, R. T. Lahey, Jr., and J. E. Flaherty, “Analysis of phase distribution in fully developed laminar bubbly two-phase flow”. *Int. J. Multiphase Flow* **17**, pp. 635-652 (1991).
7. T. Hibiki and M. Ishii, “Lift force in bubbly flow systems”, *Chem. Eng. Sci.* **62**, pp. 6457-6474 (2007).
8. M. Lopez de Bertodano, *Turbulent Bubbly Flow in a Triangular Duct*, Ph.D. Thesis, Rensselaer Polytechnic Institute, Troy New York (1992).
9. Y. Sato, M. Sadatomi, and K. Sekoguchi, “Momentum and heat transfer in two-phase bubble flow I”, *Int. J. Multiphase Flow* **7**, pp. 167-177(1981).
10. J. W. Hinze, *Turbulence*, McGraw-Hill, New York (1959).
11. Y. Liu, T. Roy, D.Y. Lee, M. Ishii, and J.R. Buchanan, Jr., “Experimental study of non-uniform inlet conditions and three-dimensional effects of vertical air–water two-phase flow in a narrow rectangular duct”, *Int. J. of Heat and Fluid Flow* **39**, pp. 173-186 (2013).
12. ANSYS CFX Release 14.0, *ANSYS CFX-Solver Theory Guide*, ANSYS Inc.(2011)
13. M. A. Lopez de Bertodano, R. T. Lahey Jr, and O. C. Jones, “Development of a  $k-\epsilon$  model for bubbly two-phase flow”, *ASME J. Fluids Eng.* **116**, pp. 128-134 (1994).
14. A.A. Troshko and Y.A. Hassan, “A two-equation turbulence model of turbulent bubbly flows”, *Int. J. Multiphase Flow* **27**(11), pp. 1965-2000 (2001).
15. E. Olmos, C. Gentric, C. Vial, G. Wild, and N. Midoux, “Numerical simulation of multiphase flow in bubble column reactors- influence of bubble coalescence and break-up” *Chem. Eng. Sci.* **56**, pp. 6359-6365 (2001).
16. V.V. Buwa and V.V. Ranade. Dynamics of gas-liquid flow in a rectangular bubble column: experiments and single/multi-group CFD simulations. *Chem. Eng. Sci.* **57**, 4715-4736 (2002).
17. F. Lehr, M. Millies, and D. Mewes, “Bubble-size distributions and flow fields in bubble columns”, *AIChE J.* **48** (11), pp. 2426-2443 (2002).
18. E. Olmos, C. Gentric, and N. Midoux, “Numerical description of flow regime transitions in bubble column reactors by a multiple gas phase model” *Chem. Eng. Sci.* **58**, 2113-2121 (2003).
19. T. Frank, J. Shi, and A. D. Burns, “Validation of Eulerian multiphase flow models for nuclear safety applications” *Proc. 3<sup>rd</sup> International Symposium on Two-Phase Flow Modeling and Experimentation*. Pisa, Italy (2004).
20. D. Zhang, N.G. Deen, and J.A.M. Kuipers, “Numerical simulation of the dynamic flow behavior in a bubble column: a study of closures for turbulence and interface forces” *Chem. Eng. Sci.* **61**, pp. 7593-7608 (2006).
21. Z. Sha, A. Laari, and I. Turunen, “Multi-phase-multi-size-group model for the inclusion of population balances into the CFD simulation of gas-liquid bubbly flows” *Chem. Eng. Technol.* **29**, pp. 550-559 (2006).
22. E. Krepper, B.N.R. Vanga, A. Zaruba, H.M. Prasser, and M.A. Lopez de Bertodano, “Experimental and numerical studies of void fraction distribution in rectangular bubble columns”, *Nucl. Eng. Des.* **237**, pp. 399-408 (2007).

23. D. Prabhudharwadkar, C. Bailey, M.A. Lopez de Bertodano, and J.R. Buchanan, "Two-Fluid CFD model of adiabatic air-water upward bubbly flow through a vertical pipe with a one-group interfacial area transport equation", *ASME 2009 Fluids Engineering Division Summer Meeting (FEDSM2009)*, Vail, Colorado, USA (2009).
24. D. Prabhudharwadkar, A. Vaidheeswaran, M. Lopez de Bertodano, J. Buchanan, and P. Guilbert, "Two-Fluid CFD simulations of cap bubble flow using the two-group interfacial area transport equations," *J. Comp. Mult. Flows*, Vol. 4, No. 4, pp. 363-374 (2012).